

## OPTICS

# Observation of Anderson localization in disordered nanophotonic structures

Hanan Herzig Sheinfux,<sup>1</sup> Yaakov Lumer,<sup>1</sup> Guy Ankonina,<sup>1</sup> Azriel Z. Genack,<sup>2</sup> Guy Bartal,<sup>1</sup> Mordechai Segev<sup>1\*</sup>

Anderson localization is an interference effect crucial to the understanding of waves in disordered media. However, localization is expected to become negligible when the features of the disordered structure are much smaller than the wavelength. Here we experimentally demonstrate the localization of light in a disordered dielectric multilayer with an average layer thickness of 15 nanometers, deep into the subwavelength regime. We observe strong disorder-induced reflections that show that the interplay of localization and evanescence can lead to a substantial decrease in transmission, or the opposite feature of enhanced transmission. This deep-subwavelength Anderson localization exhibits extreme sensitivity: Varying the thickness of a single layer by 2 nanometers changes the reflection appreciably. This sensitivity, approaching the atomic scale, holds the promise of extreme subwavelength sensing.

Anderson localization is the cornerstone of modern understanding of waves in disordered media (1–3). The formation of localized states, first predicted for electrons, has been studied in a variety of wave systems and has inspired an exceptionally rich domain of research (4–17). The study of Anderson localization has historically focused on disorder in systems with “large” spatial features (wavelength-scale or larger): Although the effect of very fine disorder on localization is described in the literature, it is commonly understood to be orders of magnitude weaker than in ordinary Anderson localization. This scenario is encountered for electromagnetic radiation. For wavelengths much larger than the typical feature size, the localization length diverges with asymptotically increasing wavelengths,  $\lambda$  (4, 18). This decrease in the impact of disorder in the subwavelength regime is by no means unique to Anderson localization. Indeed, it is generally believed that the impact on transport of any type of photonic structure, whether disordered or not, should wash out when the features are in the deep-subwavelength regime; rather, light should behave as though traveling through a homogeneous material, with an “effective medium” index of refraction (19). But this is not always the case—it was recently shown that simple periodic structures can show major deviations from the effective medium prescription (20, 21). This breakdown of effective medium theory was predicted to be particularly pronounced for disordered structures, where even  $\lambda/1000$  structural variations can exert a dominant influence (22).

Here we demonstrate Anderson localization of light in a random stack of deep-subwavelength dielectric layers. Naïvely, we would expect the role of nanophotonic disorder to be negligible, but the localization we observe is actually very strong, with localization lengths on the order of  $\lambda$ . The disorder in our experiment is thickness variations in layers with  $\sim\lambda/40$  thickness. We show how a 2-nm variation in just one of these layers is measurable. Moreover, although both Anderson localization and evanescence inhibit transmission separately, we show that transmission mediated by localized modes can be enhanced by as much as two orders of magnitude. All these results occur in the vicinity of the critical angle,  $\theta_c$ , and are intimately related to the presence of an exceptional point there.

Our disordered multilayer structures are deposited on a rutile prism whose index of refraction ( $n_{\text{TiO}_2} \sim 2.6$ ) is larger than the (calculated) effective medium of the multilayer stack (Fig. 1A). Consequently, there exists a critical angle  $\theta_c$  above which light, in the effective medium picture,

should undergo total internal reflection. The multilayer stack is composed of alternating high- and low-refractive index layers of random thickness (23) (Fig. 1, B and C). The high-refractive index layers are  $\text{Nb}_2\text{O}_5$  (bright layers), with  $n_{\text{Nb}_2\text{O}_5} \sim 2.2$  and thicknesses randomly drawn from a rectangular distribution between 6 and 30 nm. The low-refractive index layers are  $\text{SiO}_2$  (dark layers), with  $n_{\text{SiO}_2} \sim 1.5$  and random thicknesses between 5 and 15 nm. The structure consists of 180 dielectric layers with overall thickness of 2.61  $\mu\text{m}$  and average layer thickness of 14.5 nm. The multilayer is terminated by a Pt layer with  $n_{\text{Pt}} \sim 2.3$  and an absorption coefficient  $k_{\text{Pt}} \sim 4.1$ . We measure the reflection as a function of incidence angle  $\theta$  at several wavelengths and polarizations and thereby determine how much light is transmitted through the multilayer stack and coupled into the absorbing Pt.

Consider first the reflection from a structure free of disorder, where we expect the effective medium theory to describe transmission well. This periodic structure can be treated as a Fabry-Perot-like cavity filled with the appropriate  $n_{\text{eff}}(\theta, \lambda)$  and terminated with an absorbing Pt layer, with a polarization dependent  $n_{\text{eff}}$  (23). The reflection calculated for the disorder-free structure (Fig. 2A, cyan curve) exhibits regular oscillations—well-ordered peaks that become higher and denser as  $\theta$  approaches  $\theta_c$ . For  $\theta > \theta_c$ , light undergoes total internal reflection.

The reflection measured from the actual structure containing deep-subwavelength disorder (Fig. 2A, red curve) exhibits a complex and irregular pattern of dips and peaks, which differ decidedly from the effective-medium response of the disorder-free structure. Notably, for most angles of incidence smaller than  $\theta_c$ , the disordered structures are considerably more reflective, indicating that light penetrates less through the structure into the Pt layer and experiences less loss. That is, the presence of disorder, even at  $\lambda/40$  scale, has a major impact on the observed reflection. To verify that this is indeed due to disorder, we also studied an intermediate case of a weakly disordered structure. Reflection from this structure (Fig. 2A, black curve) is more irregular and more highly reflective than the disorder-free sample, but less so than the strong-disorder sample. Because this structure is

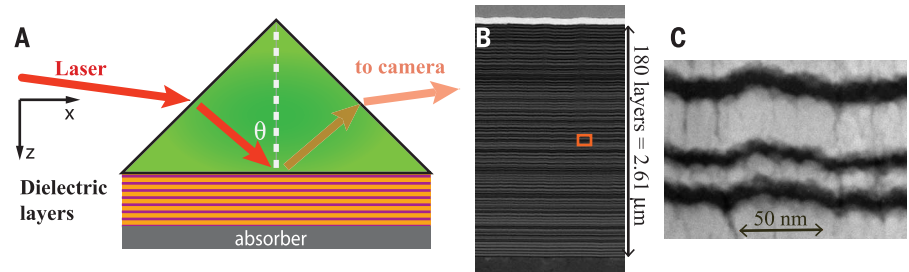


**Fig. 1. Deep-subwavelength dielectric multilayer structure and experimental apparatus.**

(A) The multilayer stack is grown on a prism and covered with an absorbing Pt layer. A laser beam is incident at angle  $\theta$  on the prism, and the output reflection is measured by a camera. (B) Transmission electron microscopy scan of a vertical cut of the multilayer showing, from bottom to top, the rutile prism material, alternating dielectric layers, the Pt layer (the absorber), and free space. (C) Magnified scan of the section in the multilayer marked by the orange rectangle in (B).

<sup>1</sup>Technion, Israel Institute of Technology, Haifa 32000, Israel.

<sup>2</sup>Physics Department, Queens College and Graduate Center of the City University of New York (CUNY), Flushing, NY 11367, USA.

\*Corresponding author. Email: msegev@tx.technion.ac.il

the same as the strongly disordered one—except for the smaller variance in the layer thicknesses—the crucial role of disorder in our results is confirmed.

When approaching the critical angle from below ( $\theta < \theta_c$ ), the disorder-free sample shows deep dips in reflection, such as the dip down to  $\sim 8\%$  reflection at  $\theta \approx \theta_c - 0.6^\circ$  (marked by “1” in Fig. 2A). By contrast, reflection measured from the disordered sample in the same angular range, marked by “2” in Fig. 2, A and B, is greatly increased by disorder: For the specific parameters here, reflection reaches 99.4% for strong disorder and 91% for weak disorder. The corresponding localization length for the strong-disorder sample is estimated (from the red curve in Fig. 2A) to be smaller than  $2\lambda$  [see (23) for details], comparable to the shortest localization length measured in any disordered electromagnetic system (24).

Another important experimental feature, which deviates sharply from the effective medium prediction, is the narrow reflection dip at  $\theta = \theta_c + 0.34^\circ$  (in the strongly disordered sample, marked

by “3” in Fig. 2A) that appears only for the strong disorder. Because this angle is larger than  $\theta_c$ , transmission should be strongly quenched with only  $3 \times 10^{-5}$  of the incident light power tunneling through the disorder-free structure. This is evident in Fig. 2C, where the disorder-free plot (cyan) is virtually flat with near-unity reflection. The 8% dip in reflection from the strongly disordered structure therefore corresponds to an enhancement in transmission of 8%. This is highly unusual, because disorder generally impedes transport (2) rather than enhancing transmission, as is seen in Fig. 2C. This enhancement disappears for weaker disorder. Transmission is enhanced by the coupling to a resonant localized mode that bridges the gap created by evanescent decay (22). On the basis of the measured reflection, we can reproduce the shape of the mode responsible for the transmission enhancement (Fig. 3A) and estimate its Q-factor to be 140 (23).

Next, we studied how transmission is modified by changes to the structure. The reflection curves in different realizations of disorder exhibit com-

pletely different angular variation. Likewise, the reflection curve is changed by altering the wavelength (Fig. 3B) or polarization (23) of the light. Although such sensitivity to deep-subwavelength modulations is unusual, we wished to take it further by asking if nanometric variations to a single layer in the structure would substantially influence the reflection.

To this end, we fabricated several multilayer structures, identical except for a single silica layer in the middle of the structure, layer number 99 (out of 180). These structures are as follows: multilayer [A], with  $d_{99}^a = 8$  nm (the measurements reported above were for multilayer [A]); multilayer [B], with  $d_{99}^b = 10$  nm; and multilayer [C], with  $d_{99}^c = 20$  nm. Ordinarily, a 2-nm difference in thickness (roughly six atoms thick) between structures [A] and [B] would be nearly indistinguishable optically. But, as can be seen in Fig. 4A, reflection measured from multilayers [A] and [B] can easily be differentiated. Most notably, the reflection dip near  $\theta = \theta_c - 1.2^\circ$  changes by 6.5%, and the enhanced transmission dip shifts. These deviations are further amplified in multilayer [C]—for example, there is a 38% difference in reflection between multilayers [A] and [C] around  $\theta = \theta_c - 2.8^\circ$ . Also shown is a “control multilayer,” [A’], which is identical to multilayer [A], including the 99th layer. The reflection curves from multilayers [A] and [A’] overlap closely, with a maximal deviation of  $\sim 3\%$ , much smaller than the differences between multilayers [A] and [B]. We conclude, therefore, that the measured differences between structures [A] and [B] are well outside the margin of fabrication and measurement error.

Finally, in Fig. 4B, we compare our measurements for the strongly disordered structure (red curve) with transfer matrix calculations (black curve). The measured reflection is generally higher than calculated, but the measurements otherwise follow the calculations closely. Namely, the calculation captures the shape of the curve and the location of the dips. The quality of this fit is even more noteworthy considering that our complex sample contains substantial fabrication imperfections, whereas the calculations are performed for an idealized multilayer stack of perfectly flat layers. For example, the multilayer exhibits surface roughness or “waviness” that can exceed the thickness of some of the layers. The quality of the agreement between measurements and calculations is therefore indicative of the robustness of this localization regime. It is extremely sensitive to longitudinal disorder, but relatively insensitive to transverse disorder.

These experimental observations are also supported by full-wave simulations [see (23)], but although the calculations seem to capture the physics involved, they provide little to understanding the underlying physics. To paint a fuller physical picture, we point to the existence of an exceptional point (EP) exactly at  $\theta_c$ . Generally, EPs occur in non-Hermitian systems when two eigenstates coalesce (25–30) and are associated with extreme sensitivity to perturbations (28). Although EPs in optics are often found in systems containing

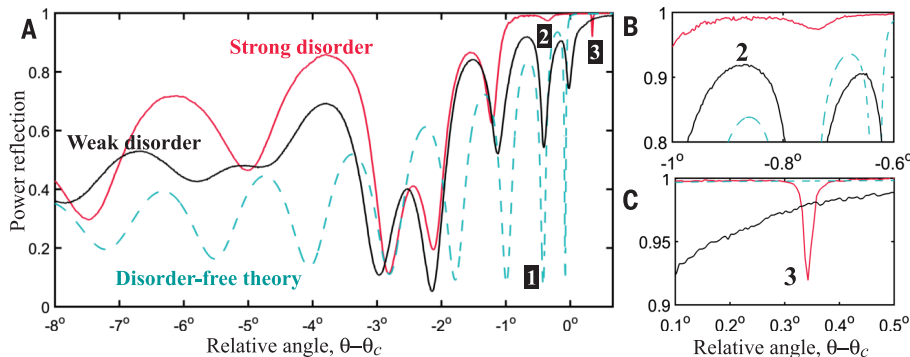


**Fig. 2. Measured reflection compared with effective medium calculation.** (A) The red and black curves are the measured reflection of transverse-magnetic polarized light from the strong disorder and weak disorder structures versus angle of incidence relative to the critical angle. Dashed cyan curve denotes calculated reflection from a disorder-free structure. The numbers 1, 2, and 3 on the plots indicate, respectively, (1) a sharp 8% dip predicted for the disorder-free case; (2) a disorder-induced reflection peak, above 99%, measured at the same angle for which effective medium theory predicts the dip marked by 1; and (3) a narrow dip corresponding to disorder-enhanced transmission at  $\theta > \theta_c$ , where the disorder-free case predicts total internal reflection. (B) and (C) are magnified views of the regions marked by 2 and 3 in (A).

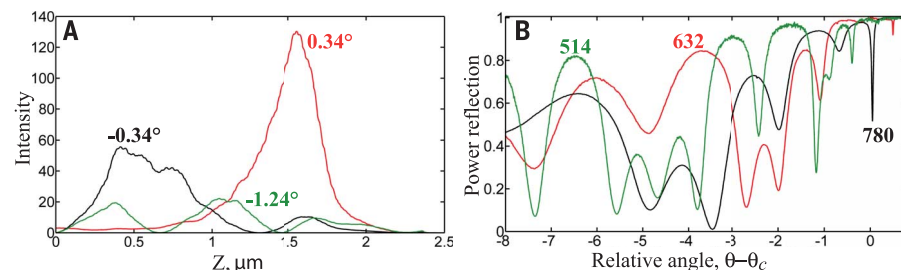


**Fig. 3. Localized modes, measurement at varying wavelengths.** (A) Calculated modes for  $\theta - \theta_c = 0.34^\circ, -0.34^\circ$ , and  $-1.24^\circ$ . These modes are responsible for the first three dips in Fig. 2A (from the right) measured for the strong-disorder structure. Specifically, the red curve shows the transmission enhancement mode. (B) Reflection measured for transverse-magnetic polarized light at several wavelengths: 514 nm (green line), 632 nm (red line), and 780 nm (black line). Changing the wavelength changes the response of the structure in a complex way.

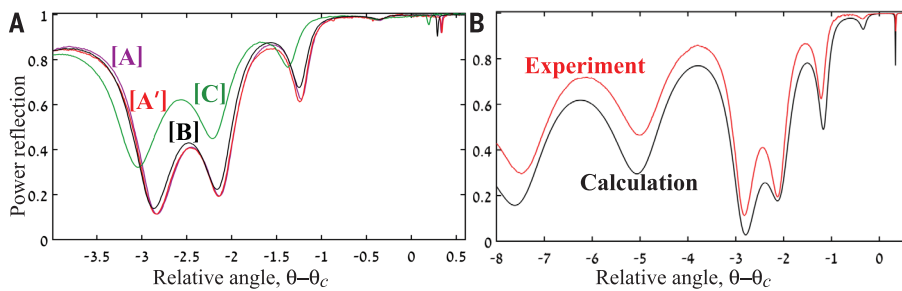


**Fig. 4. Optical sensing of 2-nm variation with deep-subwavelength disordered multilayer structure.** (A) Reflection from four structures prepared in a nearly identical fashion except for layer 99, a silica layer, with a thickness of 8 nm in multilayers [A] and [A'] (purple and red lines, respectively); 10 nm in multilayer [B] (black line); and 20 nm in multilayer [C] (green line). The reflection from multilayer [A] is easily distinguished from multilayers [B] and [C]. Notably, the distinction between multilayers [A] and [B] shows sensitivity to a 2-nm-thickness difference in one of the layers in the multilayer. By contrast, the reflection in the test-case multilayer [A'] is nearly identical to the reflection from multilayer [A], showing the robustness of reflection in the face of inevitable fabrication errors. (B) Comparison of measured reflection from the strongly disordered structure multilayer [A] (red) and transfer matrix calculation (black), showing the predictive power of transfer matrix theory, despite the inevitable presence of fabrication errors.

gain and loss (25–27), they can appear in systems with a purely real refractive index at the transition point from propagating to evanescent behavior (29, 30). In our case, we find that an EP occurs near  $\theta_c$  for a periodic multilayer structure. The presence of this EP should therefore result in extreme sensitivity to structural variations, such as the addition of a subwavelength disorder. We conjecture that this EP is the origin of the sensitivity that our disordered structures exhibit near the EP (near  $\theta_c$ ), an explanation that can also be applied to earlier findings (20–22).

Our findings—the experimental observation of Anderson localization in deep-subwavelength disordered structures—offer fundamental insights into Anderson localization and the interplay between disorder and evanescence. Beyond demonstrating the potency of localization in this regime, we also demonstrate disorder-enhanced transport and unprecedented sensitivity to 2-nm variations in the thickness of a single layer within a disordered structure. This sensitivity may be interpreted in terms of the non-Hermitian nature of the wave near an EP, but at the same time, they raise further fundamental questions related to the

features of EPs in finite and disordered systems. For example, if controllable gain and loss are added to such a disordered multilayer, will we obtain a geometric phase when the EP is encircled in phase space? We believe that the extreme sensitivity we observed here will lend itself to important applications in sensing of nanometric features and in optical switching. In particular, it is important to consider combining this disorder-induced sensitivity with high-Q modes, surface plasmons, or interferometric sensing, which could further enhance sensitivity. Ultimately, the combination of these techniques might make possible the optical measurements of atomic-scale features inside a “stack” of atomic layers.

#### REFERENCES AND NOTES

1. P. W. Anderson, *Phys. Rev.* **109**, 1492–1505 (1958).
2. A. Lagendijk, B. van Tiggelen, D. S. Wiersma, *Phys. Today* **62**, 24–29 (2009).
3. M. Segev, Y. Silberberg, D. N. Christodoulides, *Nat. Photonics* **7**, 197–204 (2013).
4. S. John, *Phys. Rev. Lett.* **53**, 2169–2172 (1984).
5. H. De Raedt, A. Lagendijk, P. de Vries, *Phys. Rev. Lett.* **62**, 47–50 (1989).
6. D. S. Wiersma, P. Bartolini, A. Lagendijk, R. Righini, *Nature* **390**, 671–673 (1997).

7. M. V. Berry, S. Klein, *Eur. J. Phys.* **18**, 222–228 (1997).
8. A. A. Chabanov, M. Stoytchev, A. Z. Genack, *Nature* **404**, 850–853 (2000).
9. M. Störzer, P. Gross, C. M. Aegerter, G. Maret, *Phys. Rev. Lett.* **96**, 063904 (2006).
10. T. Schwartz, G. Bartal, S. Fishman, M. Segev, *Nature* **446**, 52–55 (2007).
11. Y. Lahini et al., *Phys. Rev. Lett.* **100**, 013906 (2008).
12. L. Levi, Y. Krivolapov, S. Fishman, M. Segev, *Nat. Phys.* **8**, 912–917 (2012).
13. S. Karbasi et al., *Nat. Commun.* **5**, 3362 (2014).
14. J. Billy et al., *Nature* **453**, 891–894 (2008).
15. M. Pasiński, D. McKay, M. White, B. DeMarco, *Nat. Phys.* **6**, 677–680 (2010).
16. H. Hu, A. Strybulevych, J. H. Page, S. E. Skipterov, B. A. van Tiggelen, *Nat. Phys.* **4**, 945–948 (2008).
17. S. Gréillon et al., *Phys. Rev. Lett.* **82**, 4520–4523 (1999).
18. P. Sheng, B. White, Z.-Q. Zhang, G. Papanicolaou, *Phys. Rev. B* **34**, 4757–4761 (1986).
19. W. Cai, V. Shalae, *Optical Metamaterials: Fundamentals and Applications* (Springer, 2010).
20. H. Herzig Sheinfux, I. Kaminer, Y. Plotnik, G. Bartal, M. Segev, *Phys. Rev. Lett.* **113**, 243901 (2014).
21. S. V. Zhukovsky et al., *Phys. Rev. Lett.* **115**, 177402 (2015).
22. H. Herzig Sheinfux, I. Kaminer, A. Z. Genack, M. Segev, *Nat. Commun.* **7**, 12927 (2016).
23. See supplementary materials.
24. Z. Daozhong et al., *Phys. Rev. B* **50**, 9810–9814 (1994).
25. K. G. Makris, R. El-Ganainy, D. N. Christodoulides, Z. H. Musslimani, *Phys. Rev. Lett.* **100**, 103904 (2008).
26. S. Klaiman, U. Günther, N. Moiseyev, *Phys. Rev. Lett.* **101**, 080402 (2008).
27. C. E. Rüter et al., *Nat. Phys.* **6**, 192–195 (2010).
28. N. Moiseyev, *Non-Hermitian Quantum Mechanics* (Cambridge Univ. Press, 2011).
29. O. Peleg, M. Segev, G. Bartal, D. N. Christodoulides, N. Moiseyev, *Phys. Rev. Lett.* **102**, 163902 (2009).
30. B. Alfassi, O. Peleg, N. Moiseyev, M. Segev, *Phys. Rev. Lett.* **106**, 073901 (2011).

#### ACKNOWLEDGMENTS

The research of H.H.S. and M.S. was supported by the German-Israeli Deutsch-Israelische Projektkooperation (DIP) program, the U.S. Air Force Office of Scientific Research, and the Israeli ICore Excellence Center “Circle of Light.” The research of A.Z.G. was supported by National Science Foundation grant DMR/BSF-1609218. All authors contributed to all aspects of this work.

#### SUPPLEMENTARY MATERIALS

www.sciencemag.org/content/356/6341/953/suppl/DC1  
Materials and Methods  
Supplementary Text  
Figs. S1 to S10  
References (31–35)

31 July 2016; resubmitted 29 January 2017  
Accepted 4 May 2017  
10.1126/science.aah6822

## Observation of Anderson localization in disordered nanophotonic structures

Hanan Herzig Sheinfux, Yaakov Lumer, Guy Ankonina, Azriel Z. Genack, Guy Bartal and Mordechai Segev

*Science* **356** (6341), 953-956.  
DOI: 10.1126/science.aah6822

### Localizing light at the nanometer scale

Waves will propagate through a medium until scattering processes result in the excitation gradually dying away. Introducing disorder can affect that propagation by increasing the scattering, potentially reaching a point where transport is stopped. Typically, the length scale of the disorder is larger than the propagating waves. Herzig Sheinfux *et al.* now show that a stack of several-nanometer-thick layers of alternating high- and low-refractive-index material can result in the localization of light. Such deep-subwavelength structures could provide a route to manipulating light on the nanometer scale.

*Science*, this issue p. 953

#### ARTICLE TOOLS

<http://science.sciencemag.org/content/356/6341/953>

#### SUPPLEMENTARY MATERIALS

<http://science.sciencemag.org/content/suppl/2017/05/31/356.6341.953.DC1>

#### REFERENCES

This article cites 32 articles, 1 of which you can access for free  
<http://science.sciencemag.org/content/356/6341/953#BIBL>

#### PERMISSIONS

<http://www.sciencemag.org/help/reprints-and-permissions>

Use of this article is subject to the [Terms of Service](#)